DELPHI Collaboration

DELPHI 2002-034 CONF 568
July 9, 2002

Measurement of Trilinear Gauge Boson Couplings in e^+e^- Collisions at 189-209 GeV

Preliminary results for ICHEP02, Amsterdam

S. Andringa[1], **M. Blom**[2], **C. DeClercq**[3], **D. Fassouliotis**[4], **B. Kersevan**[5], **C. Matteuzzi**[6], **M. Nassiakou**[4], **U. Parzefall** [7], **R.L. Sekulin**[8], **M. Tobin**[9], **A. Van Lysebetten**[2,10], **O. Yushchenko**[11]

[1] LIP-IST-FCUL, Av. Elias Garcia, 14, P-1000 Lisboa, Portugal
[2] NIKHEF, Postbus 41882, NL-1009 DB Amsterdam, The Netherlands
[3] IIHE-Institut Universitaire des Hautes Energies, Pleinlaan 2, B-1050 Brussels, Belgium
[4] Institute of Nuclear Physics, N.C.S.R. Demokritos, P.O. Box 60228, GR-15310 Athens, Greece
[5] Univerza v Ljubljani, Institut Josef Stefan, Jamova 39, P.O.B 3000, SI-1001 Ljubljana, Slovenia
[6] Dipartimento di Fisica, Università di Milano and INFN, Via Celoria 16, I-20133 Milan, Italy
[7] CERN, CH-1211 Geneva 23, Switzerland
[8] Rutherford Appleton Laboratory, Chilton, Didcot OX11 OQX, UK
[9] Department of Physics, University of Liverpool, P.O. Box 147, Liverpool L69 3BX, UK
[10] DAPNIA/Service de Physique des Particules, CEA-Saclay, FR-91191 Gif-sur-Yvette Cedex, France
[11] Inst. for High Energy Physics, Serpukhov P.O. Box 35, Protvino, Russian Federation

Abstract

Preliminary measurements of the trilinear gauge boson couplings $WW\gamma$ and WWZ are presented from data taken by DELPHI at energies ranging from 189 to 209 GeV. Values are determined for Δg_1^Z and $\Delta\kappa_\gamma$, the differences of the WWZ charge coupling and of the $WW\gamma$ dipole couplings from their Standard Model values, and for λ_γ, the $WW\gamma$ quadrupole coupling. The study uses data from the final states $jj\ell\nu$, $jjjj$, jjX and ℓX, where j represents a quark jet, ℓ an identified lepton and X missing four-momentum. The observations are consistent with the predictions of the Standard Model.

1 Introduction

This study of trilinear gauge boson couplings (TGCs) uses data from the final states $jj\ell\nu$, $jjjj$, jjX and ℓX, where j represents a quark jet, ℓ an identified lepton and X missing four-momentum, taken by the DELPHI detector at LEP from 1998 to 2000 at centre-of-mass energies ranging from 189 GeV to 209 GeV. The data are used to determine values of three coupling parameters at the WWV vertex (with $V \equiv \gamma, Z$): Δg_1^Z, the difference between the value of the overall WWZ coupling strength and its Standard Model prediction; $\Delta\kappa_\gamma$, the difference between the value of the dipole coupling, κ_γ, and its Standard Model value; and λ_γ, the $WW\gamma$ quadrupole coupling parameter. In the evaluation of the WWV couplings, a model has been assumed [1] in which contributions to the effective WWV Lagrangian from operators describing possible new physics beyond the Standard Model are restricted to those which are CP-conserving, are of lowest dimension (≤ 6), satisfy $SU(2) \times U(1)$ invariance and have not been excluded by previous measurements. This leads to possible contributions from three operators, $\mathcal{L}_{W\phi}$, $\mathcal{L}_{B\phi}$ and $\mathcal{L}_W$, and hence to relations between the permitted values of the $WW\gamma$ and WWZ couplings: $\Delta\kappa_Z = \Delta g_1^Z - \frac{s_w^2}{c_w^2}\Delta\kappa_\gamma$, $\lambda_Z = \lambda_\gamma$, where s_w and c_w are the sine and cosine of the electroweak mixing angle. The parameters we determine are related to possible contributions $\alpha_{W\phi}$, $\alpha_{B\phi}$ and α_W from the three operators given above by: $\Delta g_1^Z = \alpha_{W\phi}/c_w^2$, $\Delta\kappa_\gamma = \alpha_{W\phi} + \alpha_{B\phi}$, and $\lambda_\gamma = \alpha_W$.

The WWV coupling arises in WW production through the diagrams involving s-channel exchange of Z or γ. We study this reaction in the final states $jj\ell\nu$, where one W decays into quarks and the other into leptons, and $jjjj$, where both Ws decay into quarks.

In single W production, the dominant amplitude involving a trilinear gauge coupling arises from the radiation of a virtual photon from the incident electron or positron, interacting with a virtual W radiated from the other incident particle. This process, involving a $WW\gamma$ coupling, contributes significantly in the kinematic region where a final state electron or positron is emitted at small angle to the beam and is thus likely to remain undetected in the beam pipe. The decay modes of the W give rise to two final states: that with two jets and missing energy (jjX), and that containing only a single visible lepton coming from the interaction point and no other track in the detector (ℓX).

The next section of this note describes the selection of events from the data and the simulation of the various channels involved in the analysis, and section 3 describes the methods used in the determination of coupling parameters. In section 4 the results from different channels are presented and combined to give overall values for the coupling parameters. A summary is given in section 6.

2 Event selection and simulation

The present analysis combines the measurements performed by DELPHI from 1998 to 2000 at centre-of-mass energies from 189 to 209 GeV. The data are divided into seven different energy bins. The separate luminosity-weighted energies and respective integrated luminosities are listed in table 1. The integrated luminosities for different selections vary slightly due to different requirements on the quality of the data. During the last part of the data-taking, at average energy of 206.7 GeV, one sector of DELPHI's main tracking

device, the time projection chamber, became inoperative. The integrated luminosities for the periods with this sector on and off are entered separately in the table.

Energy [GeV]	Hadronic [pb^{-1}]	Leptonic [pb^{-1}]
188.63	154.2	153.8
191.58	25.2	24.9
195.52	76.2	73.0
199.52	82.7	83.0
201.64	40.0	40.0
204.9	73.4	69.1
206.7	85.5	79.8
206.7*	49.5	50.0

Table 1: Energies and integrated luminosities of the data samples used in the analysis. Hadronic data corresponds to the topology $jjjj$, leptonic data to $jjl\nu$. The last row gives values for the data collected when one sector of the time projection chamber was inoperative.

We describe here the main features of the selection of events in the final state topologies defined in the previous section. A detailed description of the DELPHI detector may be found in [2], which includes descriptions of the main components of the detector used in this study, namely, the trigger system, the luminosity monitor, the tracking system in the barrel and forward regions, the muon detectors, the electromagnetic calorimeters and the hermeticity counters. The track selection and lepton identification criteria and a description of the luminosity measurement are described in [3].

Selection of events in the $jj\ell\nu$ topology:
Events in the $jj\ell\nu$ topology are characterized by two hadronic jets, a lepton, and missing momentum resulting from the neutrino. The lepton may be an electron or muon (coming either from W decay or from the cascade decay $W\to\tau...\to\ell...$) or, in the case of τ decays, it might give rise to a low multiplicity jet. The major backgrounds come from $q\bar{q}(\gamma)$ production and from four-fermion final states containing two quarks and two leptons of the same flavour.

The selection procedure was different to that used in our previous analyses [4, 5, 6]. A loose preselection, followed by an Iterative Discriminant Analysis [7] was used. Full details of the analysis and the performance of the selection in the separate channels $jj\mu\nu$, $jje\nu$ and $jj\tau\nu$ can be found in [8, 9], which describe the measurement of the W-pair production cross-section in DELPHI data at energies from 192 to 207 GeV.

The efficiency for the selection of $jj\ell\nu$ events was evaluated using fully simulated events and found to be between 72% and 76% for the various energies, with the efficiency highest for $jj\mu\nu$ (typically 89%), and lower efficiencies for $jje\nu$ (between 70% and 78%) and $jje\nu$ (between 57% and 63%). The total expected background contribution was around 0.8 pb.

Selection of events in the $jjjj$ topology:

As in the semileptonic channel, the selection procedure has been changed with respect to that applied in our previous analyses [5, 6]. After a loose preselection, a feed forward neural network, based on the JETNET package [10], was used to select events in the fully hadronic topology amongst the 2-fermion and 4-fermion backgrounds, which consist mainly of $Z/\gamma \to \mathrm{q\bar{q}}(g)$ and $ZZ \to \mathrm{q\bar{q}q\bar{q}}$, respectively.

Events were selected by applying an energy-dependent cut on the output of the neural network, with the cut chosen in order to maximize the product of efficiency and purity of the selection at the various energies. Typical efficiencies were in the range 86% to 90%, with background contributions of around 2.0 pb, consisting predominantly of $\mathrm{q\bar{q}}(g)$ events with gluon radiation. Details of the procedure are given in [8, 9].

At this stage in the analysis, events were forced into a 4-jet configuration. The next step in the event reconstruction was to determine which of the three possible di–jet combinations is most likely to represent the decay products of the WW pair. This was achieved with the aid of a neural network, constructed using the SNNS package [11]. For each of the three combinations a kinematic fit was performed, imposing four-momentum conservation and equality of the masses of the two di–jet pairs. The three fitted χ^2 values and the deviation of the fitted mass from the nominal mass of the W boson obtained in each fit were supplied as input to the neural network, which was trained to select the best pairing combination on that basis. A typical efficiency of 75% was achieved.

An additional problem in the analysis of the $jjjj$ state is to distinguish the pair of jets constituting the W^+ decay products from that from the W^-. This ambiguity can be partly resolved by computing jet charges from the momentum-weighted charge of each particle belonging to the jet, $Q_{\mathrm{jet}} = \sum_i q_i(\vec{p}_i \cdot \vec{T}_{\mathrm{jet}})^{0.7} / \sum_i (\vec{p}_i \cdot \vec{T}_{\mathrm{jet}})^{0.7}$, (where q_i and p_i are the charge and momentum of the particle, $\vec{T}_{\mathrm{jet}}$ represents the unit vector in the reconstructed jet direction, and the exponent 0.7, is chosen empirically). The $W^{\pm}$ charges, Q_{W^+} and Q_{W^-}, are then defined as the sums of the charges of the two daughter jets. Following the method of [12], the distribution of the difference $\Delta Q = Q_{W^-} - Q_{W^+}$ was then used to construct an estimator $P(\Delta Q)$ of the probability that the pair with the more negative value of Q_W is a W^-, and the variable $x_q = P_{W^-}(\Delta Q)\cos\theta_W - (1 - P_{W^-}(\Delta Q))\cos\theta_W$ (with θ_W denoting the polar angle of the di–jet pair) was constructed for use in the likelihood fit estimation.

An estimate of the efficiency of this procedure was made (for the same sample of simulated WW events as was used to estimate the jet pairing efficiency) by flagging the jet pairs with $\Delta Q < 0$ as W^- and comparing with the generated information. In order to separate this estimate from that for the efficiency of W pair assignment, only events with correct jet pairing were included in the comparison, leading to a value of $75.6 \pm 0.4\%$ for the W charge tagging efficiency.

Selection of events in the jjX topology:
Events were selected as candidates for the jjX topology if they had total measured transverse momentum greater than 20 GeV/c and invariant mass of detected particles between 45 and 90 GeV/c^2. The detected particles were clustered into jets, and events were accepted if they had two or three reconstructed jets. Surviving events were then forced into a 2-jet configuration. The selection was identical to the one used at 189 GeV and is described in detail in [6].

Selection of events in the ℓX topology:

In the selection of candidates for the ℓX final state, events were required to have only one charged particle, clearly identified as a muon from the signals recorded in the barrel or forward muon chambers or as an electron from the signals in the barrel or forward electromagnetic calorimeters. As for the jjX channel, the selection was the same as applied in our analysis at 189 GeV [6].

Event simulation:

In the study of the $jj\ell\nu$ and $jjjj$ channels, the four-fermion generator WPHACT [13], interfaced to the JETSET hadronization model [14], was used. A detailed description of the setup used in DELPHI for four-fermion event generation can be found in [15]. It incorporates the $O(\alpha)$ Double Pole Approximation radiative corrections to the doubly resonant WW production diagrams in the form provided by the YFSWW generator [16]. This represents the first application of this new theoretical work to DELPHI results on gauge couplings, shown to be necessary at the level of precision obtained with the final LEP results.

The study of backgrounds due to $q\bar{q}(\gamma)$ production was made using fully simulated events from the PYTHIA [17] and KK2F [18] models. WPHACT was used in the simulation of events from ZZ production. Two-photon backgrounds were studied using the generators of Berends, Daverveldt and Kleiss [19] and with the TWOGAM generator [20].

Fully simulated events in the single W channels were produced using the GRC4F program [21].

3 Methods used in the determination of the couplings

The existence of anomalous TGCs leads to a change both in the total cross-section of the processes we consider and in the shape of the differential distributions, - in the case of WW production, most notably in the W^- production angle. All the analyses we report make use of the total number of observed events, and differential information was also used in all of them apart from the one applied to the ℓX channel.

Data in both the $jj\ell\nu$ and $jjjj$ channels were analyzed using methods based on angular observables. For events in the $jj\ell\nu$ topology, a binned maximum likelihood fit was made to the joint distribution in three well-measured variables: the W^- production angle ($\cos\theta_W$), the polar angle of the produced lepton with respect to the incoming $e^\pm$ of the same sign and the cosine of the angle between the lepton and the W direction. In the $jjjj$ topology, the analysis involved a binned extended maximum likelihood fit to the distribution of the variable x_q – the jet-charge weighted W^- production angular distribution – defined in section 2 above.

In the analysis of channels corresponding to single W production, a binned maximum likelihood fit to the distribution of the angle between the two reconstructed jets was applied to events in the jjX topology, while in the ℓX topology fits of the TGC parameters were performed to the total observed numbers of events.

In the analysis of all the channels considered, the likelihood function for a given set of values $\vec{\lambda} = \{\lambda_1, \ldots, \lambda_n\}$ of parameters under consideration was evaluated by reweighting [22] the events, exploiting the fact that the differential cross-section, $d\sigma/d\vec{V}$, for any

set of phase space variables, $\vec{V}$, is quadratic in the trilinear gauge coupling parameters:

$$\frac{d\sigma(\vec{V},\vec{\lambda})}{d\vec{V}} = c_0(\vec{V}) + \sum_i c_1^i(\vec{V})\cdot\lambda_i + \sum_{i\le j} c_2^{ij}(\vec{V})\cdot\lambda_i\cdot\lambda_j\,, \tag{1}$$

where the sums in i, j are over the set $\vec{\lambda}$. Various calculations were used to determine the coefficients c_i: the combination of WPHACT and YFSWW described in [15] in the $jj\ell\nu$ and $jjjj$ topologies, while for events in single W topologies DELTGC [23] was used.

4 Results on WWV couplings

The results obtained in single-parameter fits using the methods discussed above, combined for all the energies listed in table 1, are displayed in table 2. In the fit to each coupling parameter, the values of the other parameters were held at zero, their Standard Model values. The errors quoted are purely statistical. A discusssion of systematic errors follows in section 5.

The combination of the fit results from the separate energies and the subsequent combination of the different channels were performed by adding the individual likelihood curves, with only statistical uncertainties included. It is necessary to use the likelihood functions directly in the combination, since in some cases they are not parabolic, and hence it is not possible to combine the results properly by simply taking weighted averages of the measurements. The likelihood curves corresponding to the results for the individual channels combined over the energies are shown in figure 1. Also shown is the likelihood-based combination of measurements of the individual channels including statistical uncertainties only, and the same combination after the inclusion of the systematic errors listed in table 7.

The results from simultaneous fits to two parameters are listed in tables 3 to 5; the corresponding contours measured at 68% and 95% confidence level are shown in figure 2. The fit results from the three-parameter fit are given in table 6. There is no natural way to show the full three-dimensional confidence level contours from this fit in a two-dimensional plot. Figure 3 shows a graphical representation of this fit where Δg_1^Z, $\Delta\kappa_\gamma$ and λ_γ are free parameters. For each of the three plots, a two-dimensional slice is cut out of the three-dimensional space. The slices are in turn cut at the minimum of each parameter separately. For each slice, two-dimensional contours for the other two parameters are plotted.

The procedure for the combination of likelihoods and inclusion of systematic errors used a minimization method proposed by Alcaraz [24], which has been used in the LEP TGC combinations of the four experiments ALEPH, DELPHI, L3 and OPAL [25]. The procedure is based on the introduction of an additional free parameter to take into account the systematic uncertainties, which are treated as shifts on the fitted TGC values, and are assumed to have Gaussian distributions. A minimization of the log-likelihood function was performed, varying simultaneously the TGC and systematic error parameters. The method has been compared with other procedures, such as the scaling method used previously by LEP and DELPHI, as well as the method based on Optimal Observables used by ALEPH and OPAL. It has been demonstrated [26] that the minimization method

agrees with the one based on Optimal Observables. The scaling method was shown to lead to an overestimate of the uncertainty resulting from systematic errors.

5 Systematic Uncertainties

Various sources of systematic errors exist in the different analysed channels. A list of the most important ones can be found in table 7.

For all the WW channels, the most significant contribution is the uncertainty in the radiative correction calculation itself, labelled $O(\alpha_{em})$ correction in the table. The uncertainty is presently taken to be the difference between Monte Carlo samples with and without the $O(\alpha_{em})$ corrections applied, as a reliable and applicable estimate of this uncertainty is at this time unavailable. This conservative approach makes the radiative correction uncertainty the dominant contribution. On the other hand, the theoretical uncertainty on the W pair production cross-section has been reduced to 0.5% in RacoonWW [27] and YFSWW, making the systematic effect from this source comparatively small.

Other important contributions in the $jj\ell\nu$ channel arise from the limited number of Monte Carlo events, the uncertainties in the jet finding efficiency and in the determination of the lepton charge (both estimated from comparisons of data and simulation at the Z resonance), and the uncertainty in the background contamination.

In the $jjjj$ channel, significant systematic effects arise from limited Monte Carlo statistics and from the imperfect modelling of the background. Further sizeable contributions come from the uncertainty in estimating the selection efficiency, and the hadronisation model used. The latter was obtained by applying the fragmentation models from JETSET and HERWIG [28] to a common set of generated events. A further source of systematic error is the uncertainty in the W mass measurement.

The systematic uncertainties in the single W channels, jjX and ℓX, originate from the estimation of the selection efficiency, the theoretical uncertainty in the single W production cross-section (taken to be $\pm 5\%$) and the background estimation.

In the combination of the likelihood curves, the correlations of some systematic errors between the $jj\ell\nu$ and $jjjj$ channels were taken into account. The following uncertainties were treated as fully correlated: the radiative correction, the W production cross-section and fragmentation. All others were assumed to be uncorrelated. The procedure to combine the channels and include systematic errors is described in the previous section. In figure 1 the overall effect of the systematic errors can be estimated by comparing the combined result with and without systematic erros. The uncertainty in the measurement is dominated by the limited amount of data.

6 Conclusions

Values for the WWV couplings Δg_1^Z, $\Delta\kappa_\gamma$ and λ_γ have been derived from a preliminary analysis of DELPHI data at 189-209 GeV. Results from semileptonic and hadronic decay of W pairs have been combined with those from single W production for all the energies. The following coupling values were measured at 1 standard deviation level in single parameter fits, including statistical and systematic uncertainties:

$$\begin{aligned} \Delta g_1^Z &= 0.003^{+0.039}_{-0.038} \\ \Delta\kappa_\gamma &= -0.043^{+0.099}_{-0.096} \\ \lambda_\gamma &= 0.015^{+0.045}_{-0.042} \end{aligned}$$

There is no evidence for deviations from Standard Model predictions in any of the couplings studied.

References

[1] G. Gounaris, J.-L. Kneur and D. Zeppenfeld, in *Physics at LEP2*, eds. G. Altarelli, T. Sjöstrand and F. Zwirner, CERN 96-01 Vol.1, 525 (1996).

[2] DELPHI Collaboration, P. Aarnio *et al.*, Nucl. Inst. Meth. **A303** (1991) 233, DELPHI Collaboration, P. Abreu *et al.*, Nucl. Inst. Meth. **A378** (1996) 57.

[3] DELPHI Collaboration, P. Abreu *et al.*, E. Phys. J. **C2** (1998) 581.

[4] DELPHI Collaboration, P. Abreu *et al.*, Phys. Lett. **B423** (1998) 194.

[5] DELPHI Collaboration, P. Abreu *et al.*, Phys. Lett. **B459** (1999) 382.

[6] DELPHI Collaboration, P. Abreu *et al.*, Phys. Lett. **B502** (2001) 9.

[7] T.G.M. Malmgrem, Comp. Phys. Comm. **106** (1997) 230.

[8] DELPHI Collaboration, P. Buschmann *et al., Measurement of the W-pair Production Cross-section and W Branching Ratios at* $\sqrt{s}$ *= 192 –202 GeV*, DELPHI Note 2000-039 CONF 357 (2000), contributed paper to the XXXVth Rencontres de Moriond.

[9] DELPHI Collaboration, P. Buschmann *et al., Measurement of the W-pair Production Cross-section and W Branching Ratios at* $\sqrt{s}$ *= 205 and 207 GeV*, DELPHI Note 2001-024 CONF 465 (2001), contributed paper to the XXXVIth Rencontres de Moriond.

[10] L. Lönnblad, C. Peterson, H. Pi and T. Rognvaldsson, *JETNET 3.1 - A Neural Network program for jet discrimination and other High Energy Physics triggering situations*, Dept. of Theor. Physics, University of Lund, Sweden (1995).

[11] Andreas Zell *et al*, *SNNS -Stuttgart Neural Network Simulator*, Report No. **6/95**, University of Stuttgart (1995).

[12] ALEPH collaboration, R. Barate *et al.*, Phys. Lett. **B422** (1998) 369.

[13] E. Accomando and A. Ballestrero, Comp. Phys. Commun. **99** (1997) 270; E. Accomando and A. Ballestrero, E. Maina hep-ph/0204052 (2002), to appear in Comp. Phys. Commun.

[14] T. Sjöstrand, *PYTHIA 5.7 / JETSET 7.4*, CERN-TH.7112/93 (1993).

[15] A. Ballestrero, R. Chierici, F. Cossutti and E. Migliore, *Four-fermion simulation at LEP2 in DELPHI*, (2002), in preparation, to be submitted to Comp. Phys. Commun.

[16] S. Jadach, W. Placzek, M. Skrzypek, B.F.L. Ward and Z. Was, Comp. Phys. Commun. **140** (2001) 475.

[17] T. Sjöstrand, *PYTHIA 5.719 / JETSET 7.4*, in *Physics at LEP2*, eds. G. Altarelli, T. Sjöstrand and F. Zwirner, CERN 96-01 Vol.2, 41 (1996).

[18] S. Jadach, B.F.L. Ward and Z. Was, Comp. Phys. Commun. **130** (2000) 260.

[19] F.A. Berends, P.H. Daverveldt and R. Kleiss, Comp. Phys. Commun. **40** (1980) 271, 285 and 309.

[20] S. Nova, S. Olchevski and T. Todorov, in *Physics at LEP2*, eds. G. Altarelli, T. Sjöstrand and F. Zwirner, CERN 96-01 Vol.2, 224 (1996).

[21] J. Fujimoto *et al., GRC4F*, in *Physics at LEP2*, eds. G. Altarelli, T. Sjöstrand and F. Zwirner, CERN 96-01 Vol.2, 30 (1996).

[22] G.K. Fanourakis, D.A. Fassouliotis and S.E. Tzamarias, Nucl. Inst. Meth. **A412** (1998) 465.

[23] O.P. Yushchenko and V.V. Kostyukhin, *DELTGC: A program for four-fermion calculations*, DELPHI note DELPHI 99-4 PHYS 816 (1999).

[24] J. Alcaraz, *A proposal for the combination of TGC measurements*, L3 Note 2718 (2001).

[25] LEP TGC Working Group, LEPEWWG/TGC/2002-01 (2002).

[26] R. Brunelière, *Tests on the LEP TGC combination procedures*, ALEPH 2002-008 PHYS-2002-007 (2002).

[27] A. Denner, S. Dittmaier, M. Roth and D. Wackeroth, Nucl. Phys. **B587** (2000) 67.

[28] G. Abbiendi, I.G. Knowles, G. Marchesini, M.H. Seymour, L. Stanco and B.R. Webber, Comp. Phys. Comm. **67** (1992) 465.

	Δg_1^Z	$\Delta\kappa_\gamma$	λ_γ
$jj\ell\nu$	$0.01^{+0.04}_{-0.04}$	$-0.09^{+0.10}_{-0.09}$	$0.02^{+0.05}_{-0.04}$
$jjjj$	$-0.02^{+0.08}_{-0.07}$	$0.06^{+0.21}_{-0.15}$	$-0.02^{+0.09}_{-0.07}$
$jjX + \ell X$	$0.04^{+0.28}_{-0.28}$	$0.05^{+0.12}_{-0.14}$	$0.06^{+0.24}_{-0.31}$
Combined	$0.00^{+0.04}_{-0.03}$	$-0.03^{+0.07}_{-0.08}$	$0.01^{+0.04}_{-0.04}$
Combined incl syst	$0.00^{+0.04}_{-0.04}$	$-0.04^{+0.10}_{-0.10}$	$0.02^{+0.05}_{-0.04}$

Table 2: The measured central values and one standard deviation errors obtained in the analysed channels in the single-parameter fits, and their combination. The first four results quoted for each coupling include only statistical errors; the combined result, including systematic errors, is given in the last row.

	Δg_1^Z	λ_γ
$jj\ell\nu$	$-0.05^{+0.08}_{-0.07}$	$0.07^{+0.09}_{-0.09}$
$jjjj$	$-0.03^{+0.13}_{-0.10}$	$0.0^{+0.12}_{-0.12}$
$jjX + \ell X$	$0.01^{+0.31}_{-0.29}$	$0.06^{+0.25}_{-0.34}$
Combined	$-0.01^{+0.05}_{-0.09}$	$0.03^{+0.09}_{-0.06}$
Combined incl syst	$-0.02^{+0.06}_{-0.07}$	$0.04^{+0.08}_{-0.07}$

Table 3: The measured central values and one standard deviation errors obtained in the two-parameter fit to Δg_1^Z and λ_γ, and their combination. The first four results quoted for each coupling include only statistical errors; the combined result, including systematic errors, is given in the last row.

	$\Delta\kappa_\gamma$	λ_γ
$jj\ell\nu$	$-0.12^{+0.10}_{-0.08}$	$0.04^{+0.05}_{-0.05}$
$jjjj$	$0.18^{+0.34}_{-0.23}$	$-0.08^{+0.12}_{-0.09}$
$jjX + \ell X$	$0.05^{+0.12}_{-0.15}$	$0.04^{+0.26}_{-0.27}$
Combined	$-0.03^{+0.07}_{-0.09}$	$0.01^{+0.05}_{-0.04}$
Combined incl syst	$-0.05^{+0.10}_{-0.11}$	$0.02^{+0.05}_{-0.04}$

Table 4: The measured central values and one standard deviation errors obtained in the two-parameter fit to $\Delta\kappa_\gamma$ and λ_γ, and their combination. The first four results quoted for each coupling include only statistical errors; the combined result, including systematic errors, is given in the last row.

	Δg_1^Z	$\Delta\kappa_\gamma$
$jj\ell\nu$	$0.02^{+0.04}_{-0.04}$	$-0.11^{+0.10}_{-0.08}$
$jjjj$	$-0.06^{+0.10}_{-0.07}$	$0.18^{+0.29}_{-0.23}$
$jjX + \ell X$	$0.04^{+0.26}_{-0.26}$	$0.05^{+0.13}_{-0.14}$
Combined	$0.00^{+0.04}_{-0.03}$	$-0.02^{+0.08}_{-0.08}$
Combined incl syst	$0.00^{+0.04}_{-0.04}$	$-0.05^{+0.12}_{-0.10}$

Table 5: The measured central values and one standard deviation errors obtained in the two-parameter fit to Δg_1^Z and $\Delta\kappa_\gamma$, and their combination. The first four results quoted for each coupling include only statistical errors; the combined result, including systematic errors, is given in the last row.

	Δg_1^Z	$\Delta\kappa_\gamma$	λ_γ
$jj\ell\nu$	$-0.02^{+0.06}_{-0.07}$	$-0.12^{+0.10}_{-0.09}$	$0.06^{+0.07}_{-0.07}$
$jjjj$	$-0.03^{+0.15}_{-0.11}$	$0.19^{+0.32}_{-0.24}$	$-0.05^{+0.16}_{-0.16}$
Combined	$0.00^{+0.04}_{-0.08}$	$-0.07^{+0.12}_{-0.08}$	$0.03^{+0.09}_{-0.05}$
Combined incl syst	$-0.01^{+0.05}_{-0.07}$	$-0.07^{+0.12}_{-0.10}$	$0.04^{+0.07}_{-0.06}$

Table 6: The measured central values and one standard deviation errors obtained in the analysed channels in the three-parameter fit, and their combination. The first three results quoted for each coupling include only statistical errors; the combined result, including systematic errors, is given in the last row.

Channel	Source	Δg_1^Z	$\Delta\kappa_\gamma$	λ_γ
$jj\ell\nu$	MC statistics	0.002	0.005	0.003
	Jet efficiency	0.002	0.006	0.002
	Lepton charge	0.001	0.007	0.002
	$O(\alpha_{em})$ correction	0.010	0.067	0.013
	Background	0.002	0.007	0.003
	Hadronisation	0.001	0.003	0.001
	σ_{WW} prediction	0.001	0.010	0.002
$jjjj$	MC statistics	0.045	0.093	0.052
	Efficiency	0.021	0.136	0.029
	W mass	0.012	0.024	0.014
	Luminosity	0.011	0.068	0.013
	$O(\alpha_{em})$ correction	0.063	0.157	0.068
	Background	0.025	0.081	0.029
	Hadronisation	0.032	0.078	0.041
	σ_{WW} prediction	0.006	0.038	0.008
jjX, ℓX	$\sigma_{singleW}$ prediction	0.004	0.076	0.035
	Efficiency	0.031	0.110	0.063
	Background	0.010	0.014	0.011

Table 7: Systematic uncertainties in the measurement of TGC for the channels studied

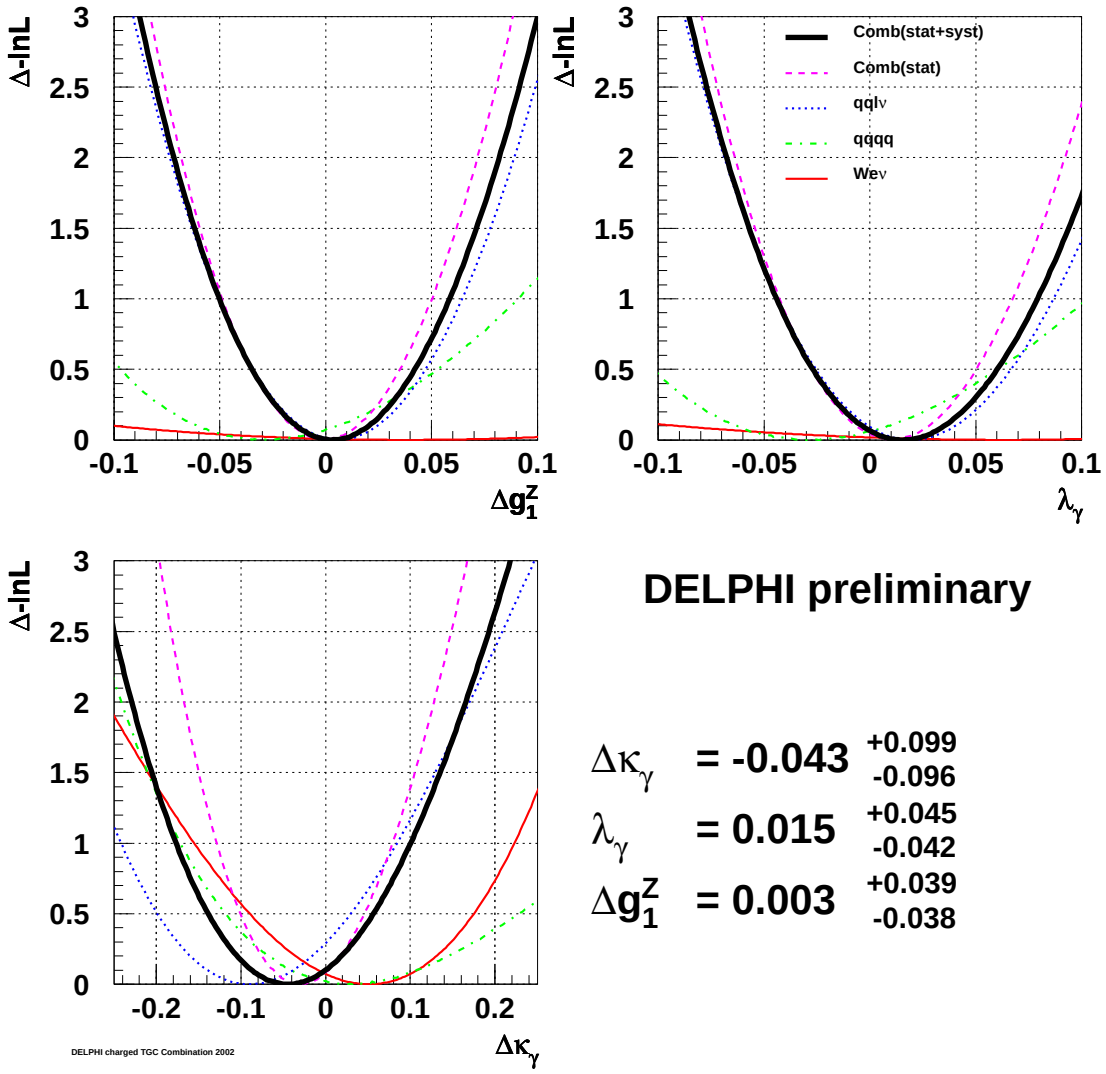

Figure 1: The likelihood curves corresponding to data from the three individual channels $e^+e^-\to W^+W^-\to qq\ell\nu$, $e^+e^-\to W^+W^-\to qqqq$ and $e^+e^-\to We\nu$, with only statistical errors included, and their combination (thin lines) for the three charged TGCs Δg_1^Z, $\Delta\kappa_\gamma$ and λ_γ. Also shown is the combined curve including statistical as well as systematic uncertainties (thick line). In each case, the minimal value is subtracted.

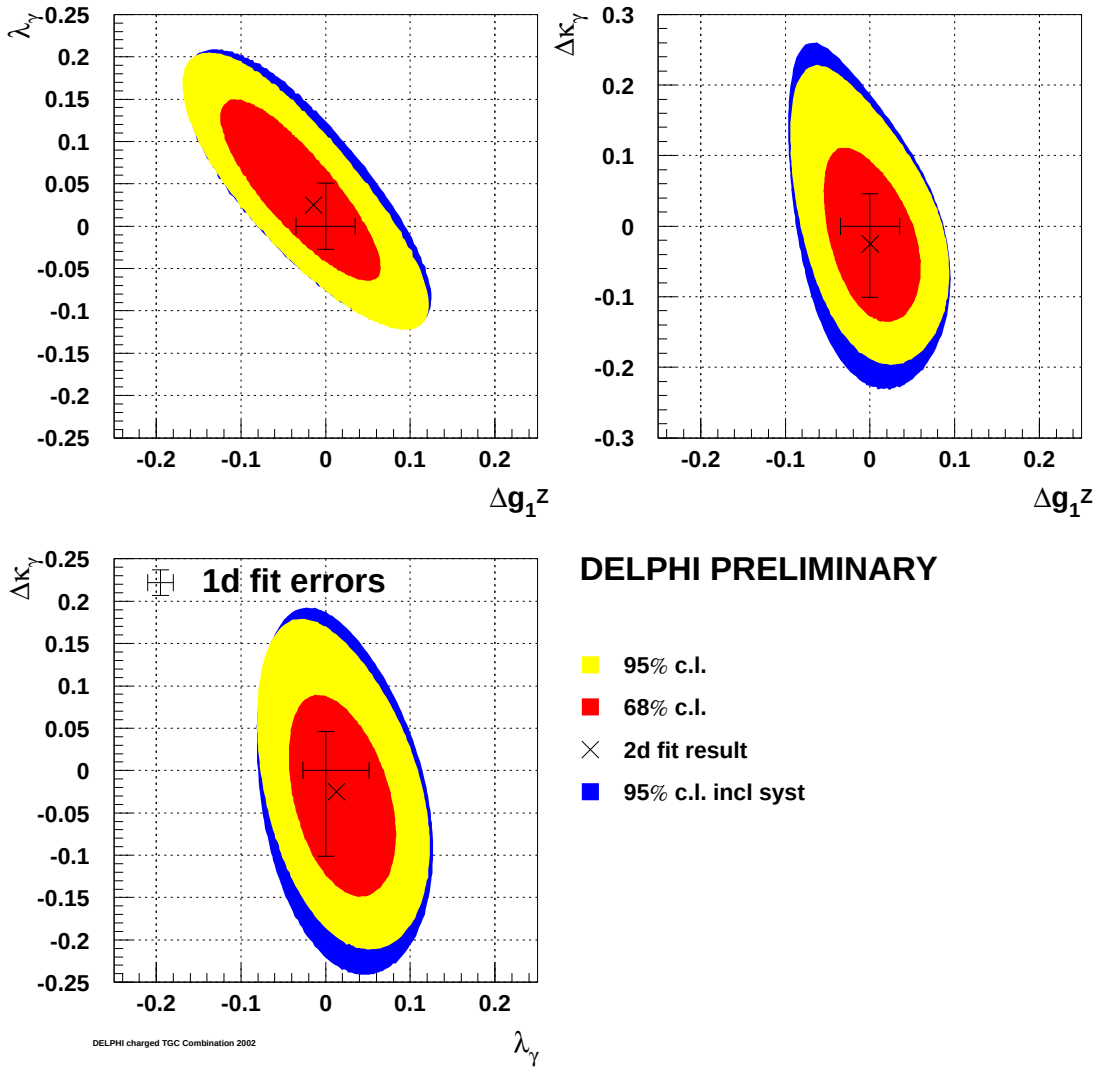

Figure 2: The results of the three two-parameter fits. For each fit, the fitted value and the contours corresponding to 68% and 95% c.l. are shown. The 1 s.d. errors obtained in the two respective single-parameter fits are superimposed on top of the 68% c.l. contour. The contours and errors described above include only statistical uncertainties. An additional 95% c.l. contour, including also systematic errors is plotted as well.

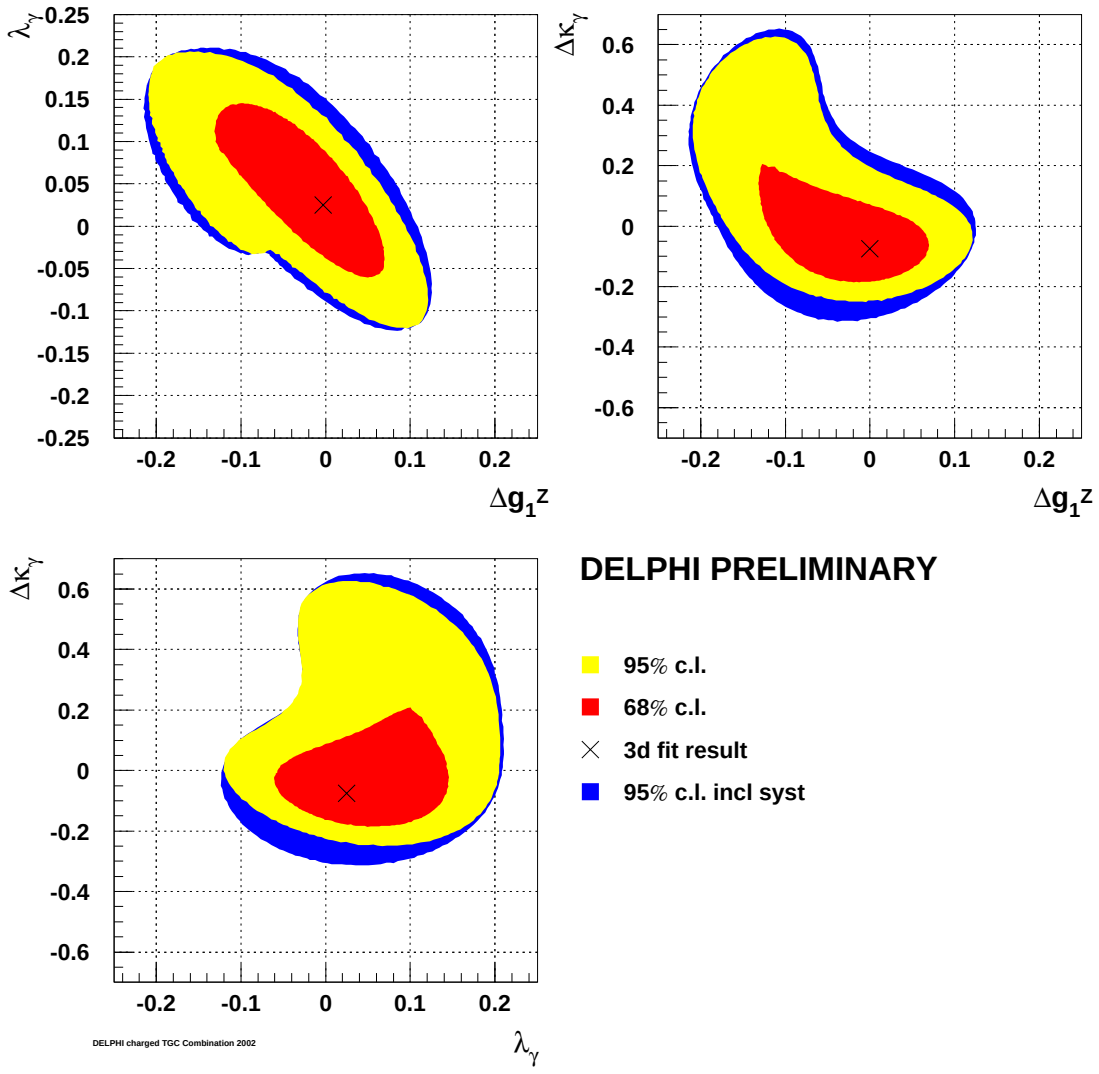

Figure 3: The result of the three-parameter fit in a two-dimensional representation. Shown are the three two-parameter contours with the third parameter at its minimum. For each pair of parameters, the fitted value and the contours corresponding to 68% and 95% c.l. are shown. The contours include only statistical uncertainties. An additional 95% c.l. contour, including also systematic errors is plotted as well.